

# Proposal of hysteresis model and damage evaluation method of steel beams subjected to inelastic cyclic loading

**K.Mori & T.Ito**

*Tokyo University of Science, Tokyo, Japan*



## SUMMARY

From the viewpoint of the suffering to the unexpected situations in the design process, it is desirable to ensure the structural performance such as a redundancy, a robustness and a repairability. The cumulative damage and residual resistant performance after inelastic response are important indexes to establish the design guideline considering these performance. In order to estimate these damage indexes, it is necessary to simulate accurately the behaviour of the structure until the ultimate states such as the buckling or the fracture of the steel members. This paper proposed the analytical methods based on the cumulative damage index which predicts the ductility at the maximum strength and the restoring force and hysteresis model. It shows a good agreement of the test results.

*Keywords: steel beam, damage evaluation, restoring force model*

## 1. INTRODUCTION

In recent years, the terrible earthquake events that were unexpected in the design process have occurred in the world, such as the 2011 off the Pacific coast of Tohoku Earthquake. From the viewpoint of the suffering to the unexpected situations, it is desirable to ensure the structural performance such as redundancy, robustness and repairability. It can be said that the cumulative damage and residual resistant performance after inelastic response are important indexes to establish the design guideline considering these ultimate states performance. In order to estimate these damage indexes, it is necessary to simulate accurately the behaviour of the structure until the ultimate states such as buckling or fracture of members.

These ultimate states of members such as buckling or fracture would cause the unstable situations on the steel members or the steel structure. And also, several analysis methods or models at the above ultimate states of the steel members have been proposed. For example, FEM analysis can simulate a strong nonlinear inelastic behaviour of members. However, these detailed analytical methods have some difficulty to use in the design process. This paper proposes a simple model and analytical methods which have high applicability and rationality about steel beams subjected to inelastic cyclic loading.

Herein, Figure 1.1 compares the hysteresis loops of analytical results which have experienced the same maximum plastic deformation. As shown in this Figure, the hysteresis behaviour is not same by the difference of the time-displacement history. From these results, it is suggested that it would be judged the same maximum plastic damage not considering the different cumulative damage experienced in the design process, but there are any questions with that.

It is widely recognized that Manson-Coffin law and Miner's law are the effective evaluation methods of the damage on steel beam subjected to constant cyclic loadings. However, in case of above random plastic cyclic loadings, these methods are restricted to adopt for the cumulative damage prediction. In this paper, the evaluation method of the cumulative fatigue damage is proposed.

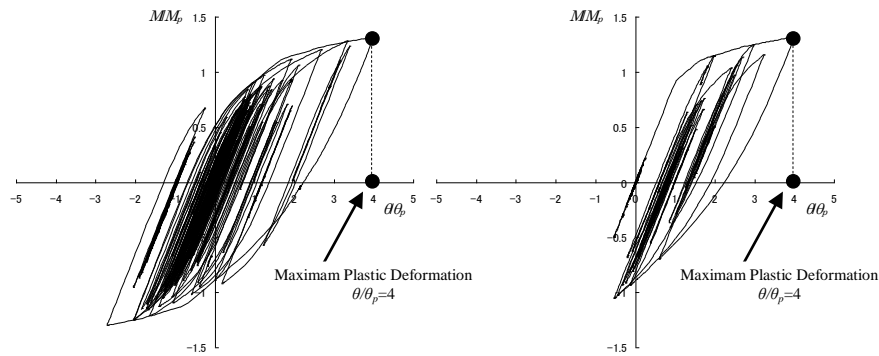


**Figure 1.1.** Comparison of hysteresis loops

## 2. OUTLINE OF DATABASE

### 2.1. Past Test Data

The strength, ductility and hysteresis loops of steel beams subjected to inelastic cyclic loadings are reviewed with a large number of past references, from which a database has been structured. Total size of test data is 134 which were reported in Japanese past papers from 1975 to 2010. A part of the database in Japanese can be downloaded from the following URL.

URL: <http://www.rs.kagu.tus.ac.jp/tito-lab/rinkD.html>

### 2.2. Material Properties, Slenderness Ratio and Width - Thickness Ratio

The yield strength, tensile strength, Young's modulus and elongations from the material test results have been stored in the database. Furthermore, the slenderness ratio and width-thickness ratio shown in past papers has been structured. However, because the slenderness ratio or width-thickness ratio weren't indicated in partly papers, these values were got by the specimen in original papers.

### 2.3. Loading Type and Path

The loading types are classified as; cantilever, pin-supported simple beam and fix-supported beam. And also, the loading paths are classified as; constant amplitude cyclic loading, gradual increase loading, and random loading.

### 2.4. Failure Mode

The failure modes observed in past papers are classified as; lateral buckling and local buckling. These failure modes shown in the papers are stored in the database.

### 2.5. Pickup Strength and Ductility on Load Deformation Curves

From the hysteresis loops of test results, the load - cumulative deformation curve is abstracted as shown in Figure 2.1. And also, the strength and ductility on the curve are picked up.

### 2.6. Consideration of Database

From the database, the relation of absorbing energy and cycle number is illustrated in Figure 2.2. From the results, it is confirmed that the absorbing energy is in a relation of the exponentiation with cycle number. In addition, it has been confirmed that the relation of other variables and test results do not show such a clear relations.

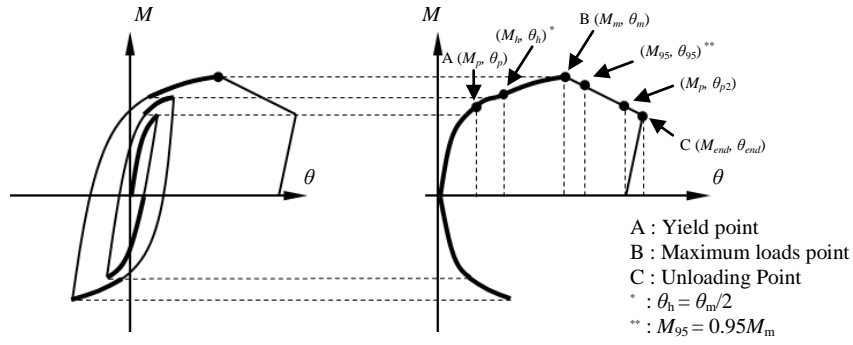


**Figure 2.1.** Pickup points of strength and ductility

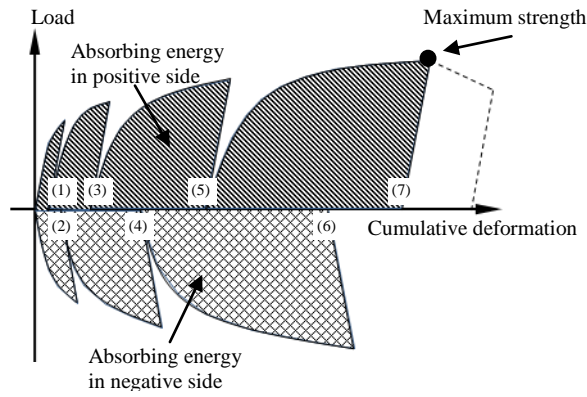


**Figure 2.2.** Relation between absorbing energy and cycle number

### 3. PROPOSAL OF DAMAGE EVALUATION METHODS AND CUMULATIVE DAMAGE INDEX

#### 3.1. Evaluation of Energy Absorbing Capacity

According to the database and Figure 2.2, the relation between energy absorption capacity and cycle number until the loads reaches the maximum strength is formulized as;

$$\frac{c\eta_m}{s\eta_m} = 2c(1-\gamma_m)N_{em}^{k+1} + 2\gamma_m - 1 \quad (3.1)$$

where  $c\eta_m$  is the cumulative plastic deformation,  $s\eta_m$  is the energy absorption capacity until the load reaches the maximum strength, and  $c, k$  are constants. Furthermore, the constants are determined from the database, and  $c = 1.26, k = -0.432$ , respectively.  $N_{em}$  is the half effective cycle number and  $\gamma_m$  is the amplitude deviation defined in next section.

##### 3.1.1 Cycle Number until Maximum Strength: $N_{em}$

In this paper, a half cycle is defined as one cycle illustrated as Figure 3.1. As shown in this figure, a half cycle over 5% energy of maximum absorbing energy is regarded as effective cycle, however, the cycle less than 5% is ignored. And also,  $N_{em}$  is defined as the sum of the effective cycle. According to this rule, a cycle with small amplitude after the large amplitude experienced is not ignored. In this example as shown in Figure 3.1, the cycle number until the load reaches the maximum strength is counted as 7, but the effective cycle number is counted as 5. The above cycle is renewed at each cycle

by consideration with the effective cycle which would cause the plastic damage.

### 3.1.2. Deviation of Amplitude until Maximum Strength: $\gamma_m$

An index  $\gamma_m$  which means the deviation of the amplitude until a load reaches the maximum strength is defined as;

$$\gamma_m = \frac{\max\{c\eta_{m(+)} \text{ } c\eta_{m(-)}\}}{c\eta_m} \quad (3.2)$$

where  $c\eta_{m(+)}$  is the absorbed energy on the positive side,  $c\eta_{m(-)}$  is the absorbed energy on the negative side as shown in Figure 2.1-(c). If the same amplitude in positive and negative side is loaded,  $\gamma_m$  becomes 0.5. And the unidirectional such as monotonic loading is loaded,  $\gamma_m$  becomes 1.0.

### 3.2. Determination Method of Unknown Parameter in Evaluation Index

To predict the  $c\eta_m$  using Eqn.(3.1), it is necessary to determine the unknown parameters ( $s\eta_m, N_{em}, \gamma_m$ ) beforehand. Herein, it is widely recognized that the skeleton curve under cyclic loaded as shown in Figure 2.1-(b) is almost similar to the load deformation curve subjected to monotonic loading. From this knowledge, the absorbed energy in the skeleton curve is determined by reference of past test results subjected to monotonic loading and the past proposed equations.

### 3.3. Formularization of Evaluation Index related to Damage

From the Eqn. (3.1), the following expression is obtained;

$$1 = \frac{1}{s\eta_m} \frac{c\eta_m}{2c(1-\gamma_m)N_{em}^{k+1} + 2\gamma_m - 1} \quad (3.3)$$

By use of an arbitrarily constant  $D$ , the index on cycle- $i$  is expressed as;

$$D = \frac{1}{s\eta_i} \frac{c\eta_i}{2c(1-\gamma_i)N_{ei}^{k+1} + 2\gamma_i - 1} \quad (3.4)$$

Furthermore, the deviation amplitude defined as Eqn. (3.2) on cycle- $i$  is expressed as;

$$\gamma_i = \frac{\max\{c\eta_{i(+)} \text{ } c\eta_{i(-)}\}}{c\eta_i} \quad (3.5)$$

From the Eqn. (3.4) and (3.5), it means that the load reaches the maximum strength when  $D$  becomes 1. And also, it means that the load increase when  $D$  is below 1, it means the strength is deteriorated when  $D$  exceeds 1.

### 3.4. Fomulari zation of Evaluation Index related to Damage

Index  $D$  about all test data is calculated, and the results are shown in Figure 5. From the Figure 5, it is observed that some of the precision of evaluation shows good, however any results shows the double or half for the test result. On the next chapter, the effects of each parameters related to evaluation and the cause of the errors are investigated in detail.

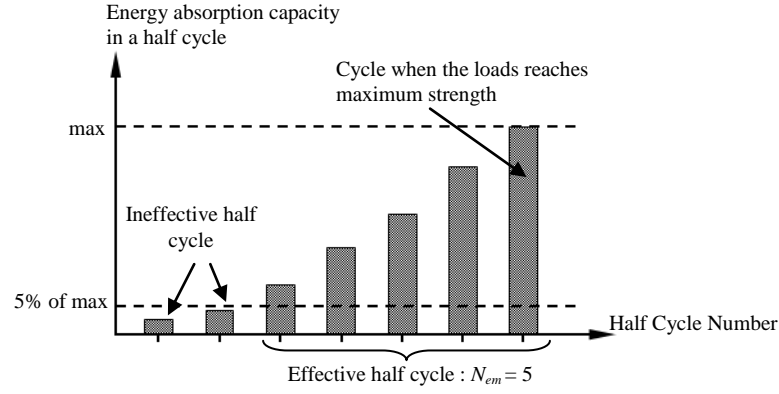


**Figure 3.1.** Example of half-cycle absorbing energy and effective cyclic number

## 4. ANALYSYS OF DAMAGE EVALUATION AND CONSIDERATION

### 4.1. Effects of Parameters Related to Damage Evaluation and Characteristics of Member

From the prior examination of database and test data of load-deformation curve,  $c\eta_m$ ,  $s\eta_m$ ,  $N_{em}$  and  $\gamma_{em}$  are recognized as an important index. Herein, these indexes are focused on the consideration of the effects of the precious prediction. Especially, the following parameters are considered as parametric studies:

- (1)  $\lambda_x$  : the general slenderness ratio
  - (2)  $\beta_{eq}$  : the equivalent width thickness ratio
  - (3)  $s\eta_m$ : the energy absorption capacity until the load reaches the maximum strength
  - (4)  $c\eta_m/s\eta_m$ : the ratio of the absorbed energy on each side to the energy absorption capacity
- where the general slenderness ratio  $\lambda_x$  is given as;

$$\lambda_x = \frac{1}{\pi} \frac{L}{i_x} \sqrt{\varepsilon_y} \quad (4.1)$$

where  $L$  is the span length,  $i_x$  is the major axis radius of gyration,  $\varepsilon_y$  is the yield strain. And the equivalent width-thickness ratio  $\beta_{eq}$  is given as;

$$\beta_{eq} = \sqrt{\left(\frac{b}{t_f}\right)^2 \varepsilon_{yf} + \left(\frac{d}{t_w}\right)^2 \frac{\varepsilon_{yw}}{41}} \quad (4.2)$$

where  $b/t_f$  is flange width thickness ratio,  $d/t_w$  is web width thickness ratio,  $\varepsilon_{yf}$ ,  $\varepsilon_{yw}$  are flange and web yield strain. And  $b$ ,  $d$  are the width of flange and web,  $t_f$ ,  $t_w$  are the thickness of flange and web, respectively.

To investigate the effects of the slenderness ratio and the width thickness ratio of the members, Figure 4.1 shows the relation of index  $D$  vs. each parameter. As shown in this figure, it can't be said that there is the clear relation each other. The reason is that the index  $D$  represented in Eqn. (3.4) does not include these parameters directly.

Furthermore, Figure 4.2 shows the relation of index  $D$  vs. the energy absorption capacity  $s\eta_m$ ,  $c\eta_m/s\eta_m$ . And also, the prediction errors of index  $D$  to test results are shown in Figure 4.2. From the Figure 4.2-(a), it is recognized that the errors of index  $D$  are increased in the low  $s\eta_m$  regions, however, the index  $D$  estimates the cumulative damage excessively. On the other hand, in the large  $s\eta_m$  region, the index  $D$  underestimates the cumulative damage.

## 4.2. Comparison of Proposed Method and Miner's Law

The Miner's law is widely recognized as the damage prediction index under the incremental and cyclic loading. Herein, the following index based on the Miner's law is applied:

$$D_M = \sum_i \frac{1}{N_{mi}} = \sum_i \left( \frac{c_c \eta_i}{c \eta_i} \right)^{\frac{1}{k}} \quad (4.3)$$

where  ${}_h\eta_i$  is the absorbed energy under half cycle,  $N_{mi}$  is the half cycle number until it reaches the maximum strength under the constant half cycle.

The comparison of the proposed method, the Miner's law of Eqn. (4.3) and test results are shown in Figure 4.3. But the Miner's law isn't shown in case 3 (Figure 4.3-(c)), because this case isn't obtained from Eqn. (4.3). From the results of Figure 4.3, the values of the D calculated by the proposed method surpass those from the rest results, i.e. the proposed method evaluates the energy absorption capacity of the test specimens on the safe side. The calculation error between the rest results and the calculated values decreases with the increase of the cycle number. The Miner's law shows the reasonable agreement with the test results in the first cycle. However, the proposed method indicates more close agreement than the Miner's law with the cycle number increases.

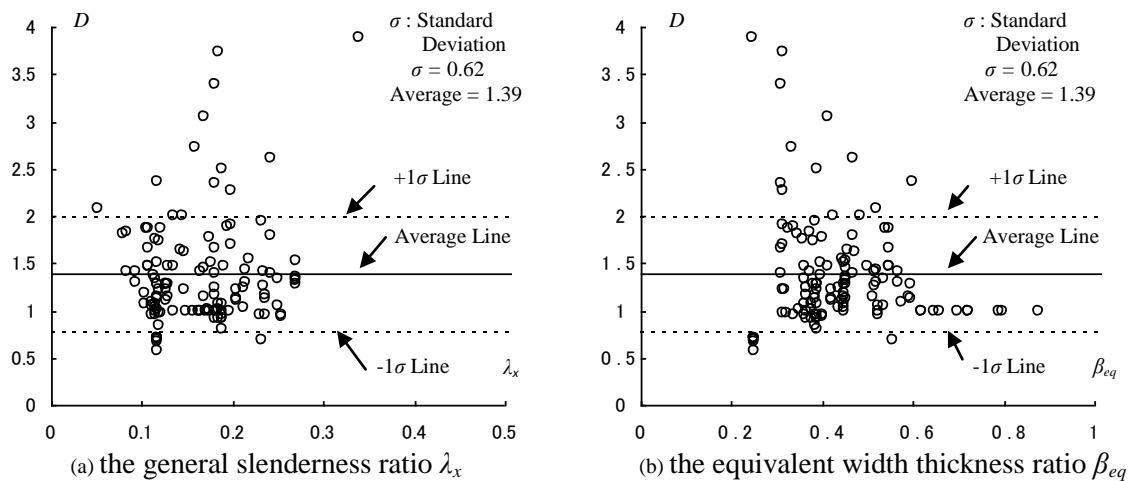


Figure 4.1. index D vs. the slenderness ratio and the width thickness ratio

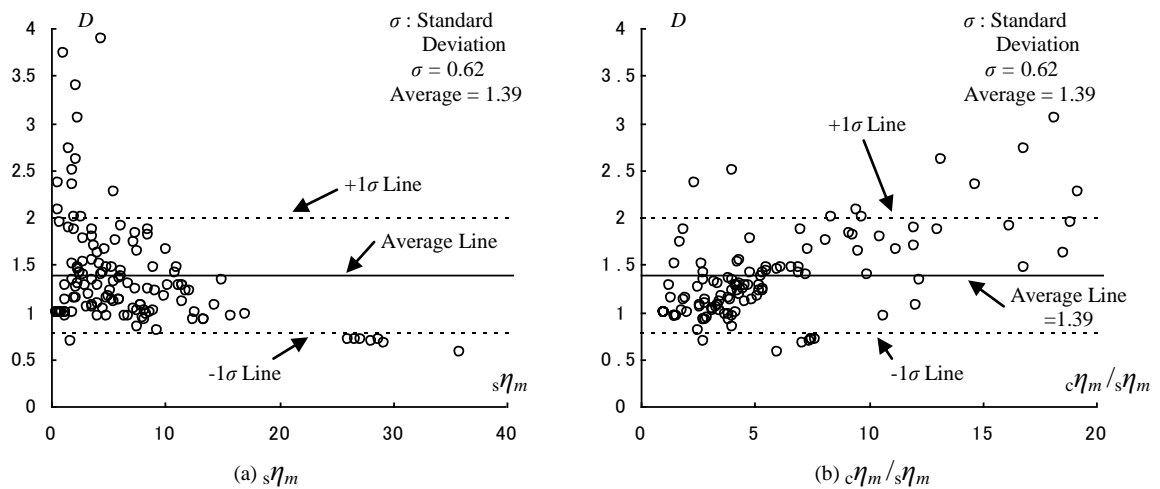


Figure 4.2. index D vs. the energy absorption capacity

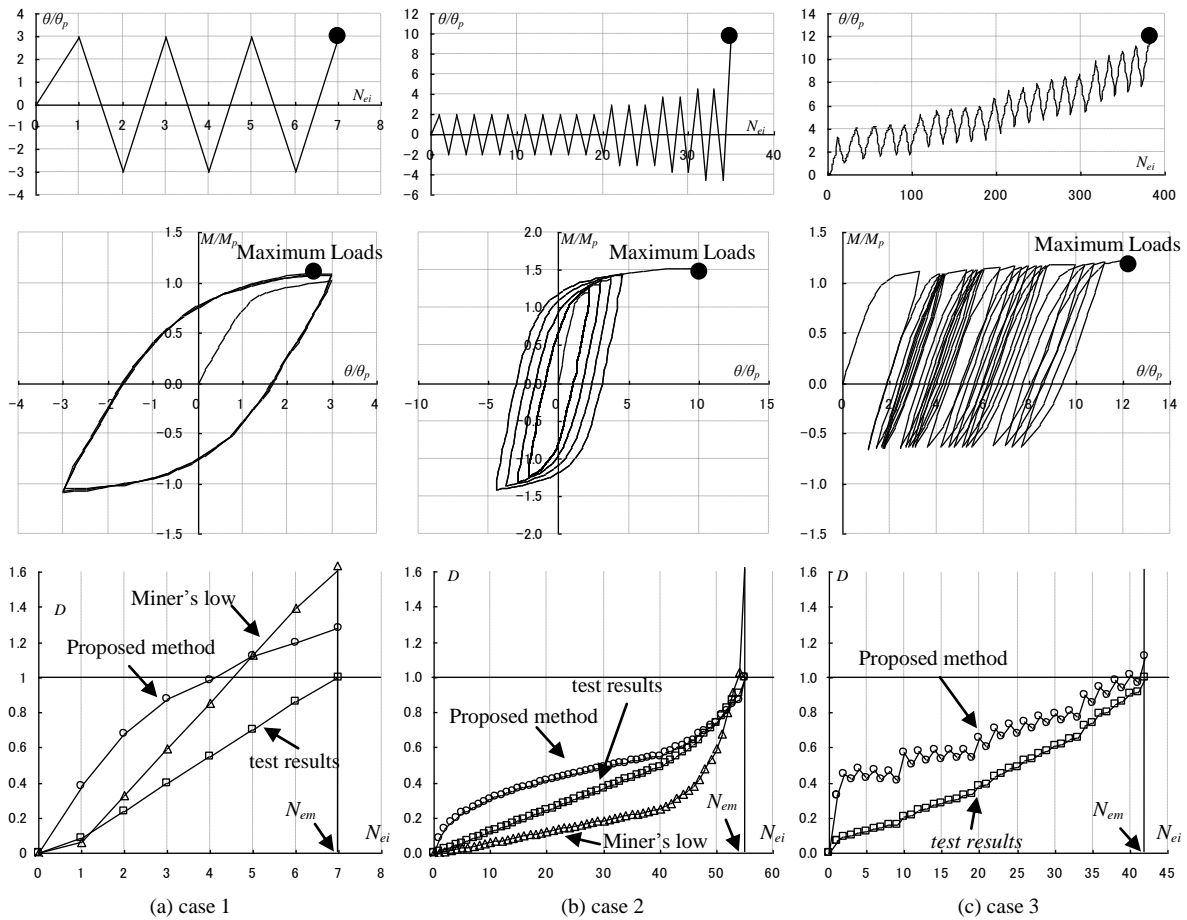


Figure 4.3. Comparison of Proposed Method and Miner's Law

## 5. PROPOSAL OF HYSTERESIS MODEL

### 5.1. Description of Skeleton Shift Model

“Skeleton Shift Model (Meng, Ohi and Takanashi, 1992)” has been proposed to express strain hardening or stress degrading phenomena of steel members under cyclic loading. In this proposed model, an original form of the skeleton curve is composed of tri-linear curve and hysteresis loops are expressed by RO model (Ramberg and Osgood, 1943). A special feature of the Skeleton Shift Model is that skeleton curve moves depending on experienced plastic strains. A model of skeleton curve and the hysteresis rule of skeleton shift model are shown in Figure 5.1.

### 5.2. Skeleton Curve

In this paper, the load-deformation curve of test data is expressed as tri-linear curve as shown in Figure 5.1-(a), and the abstracted tri-linear model is applied to the skeleton curve model for the analytical model.

### 5.3. Shift Coefficient under Cyclic Loading

On the hysteresis rule of the skeleton shift model, the skeleton curve is moved depending on the plastic deformation experienced on the opposite side as shown in Figure 5.1-(b). The shift coefficient

has not been proposed and formularized in the past papers yet. Herein, the regression equation of this shift coefficient is determined by reference of the database as;

$$\varphi = -0.355 \times \ln\{3.187 \times (100\varepsilon_y - 0.103)^{0.466} \times (\frac{c\eta_m}{s\eta_m})^{0.751} + 1\} + 1 \quad (5.1)$$

#### 5.4. Hysteresis Rule during Unloading Process

As the previous mentioned, the hysteresis loop during unloading is expressed as RO curve. However, the little errors have been pointed out in the past researches under the random loadings. Herein, to improve these errors, the following rules are proposed.

When the loci of load deformation curve moves over the outside loop, the following model is applied to modify this behaviour:

Tangent stiffness  $K^*$  on the RO curve is given as;

$$K^* = \frac{K_0 K_a}{K_a + r(K_0 - K_a) \left| \frac{P - P_u}{P_t - P_u} \right|^{r-1}} \quad (5.2)$$

where  $K_0$  is initial stiffness,  $K_a$  is secant stiffness,  $P_u$  is the unloading loads,  $P_t$  is the target loads.  $r$  is the coefficient in Ramberg-Osgood function.

The regression equation of this coefficient is determined by reference of the database as:

$$r = \frac{0.292}{\lambda_x^{0.301} \times (\beta_{eq} + 0.260)^{1.379} \times (100\varepsilon_y + 0.014)^{0.600}} + 5.176 \quad (5.3)$$

As shown in Figure 5.2-(a), when the loci of load deformation curve moves over the outside loop, the following relation hold;

$$K_t > K_t' \quad (5.4-a)$$

where  $K_t, K_t'$  is;

$$K_t = K_0 \cdot K_a / \{ K_a + r(K_0 - K_a) \} \quad (5.4-b)$$

$$K_t' = K_0 \cdot K_a' / \{ K_a' + r(K_0 - K_a') \} \quad (5.4-c)$$

$$K_a' = (P_t - P_u') / (\delta_t - \delta_u') \quad (5.4-d)$$

in which  $K_a'$  is secant stiffness between the re-unloading point and the target point,  $P_u'$  is the re-unloading loads,  $\delta_u'$  is the re-unloading deformation.

From the Eqn. (5.4), the following expression is obtained;

$$K_a > K_a' \quad (5.5)$$

To prevent the loci of load deformation curve moving over the outside loop, the hysteresis loop is modified as follows;

$$K_t = K_t' \quad (5.6)$$

Based on these calculations Eqn.(5.4) to Eqn. (5.6),  $r'$  which is the modified coefficient  $r$  is determined as follows;

$$r' = r \cdot \frac{K_a'}{K_a} \cdot \frac{K_0 - K_a}{K_0 - K_a'} \quad (5.7)$$

Also the following expression is obtained;

$$K^* = \frac{K_0 K_a'}{K_a' + r'(K_0 - K_a')} \left| \frac{P - P_u'}{P_t - P_u'} \right|^{r'-1} \quad (5.8)$$

Figure 5.2-(b) shows the hysteresis loop modified by the Eqn. (5.8).

### 5.5. Comparison of Hysteresis Loops of Test Result and Analytical Result by Proposal Method

Figure 5.3 shows the comparisons of the hysteresis loops of test results and analytical results by proposal methods. From the Figure 5.3, it is observed that the analytical model has good agreements with the test results.

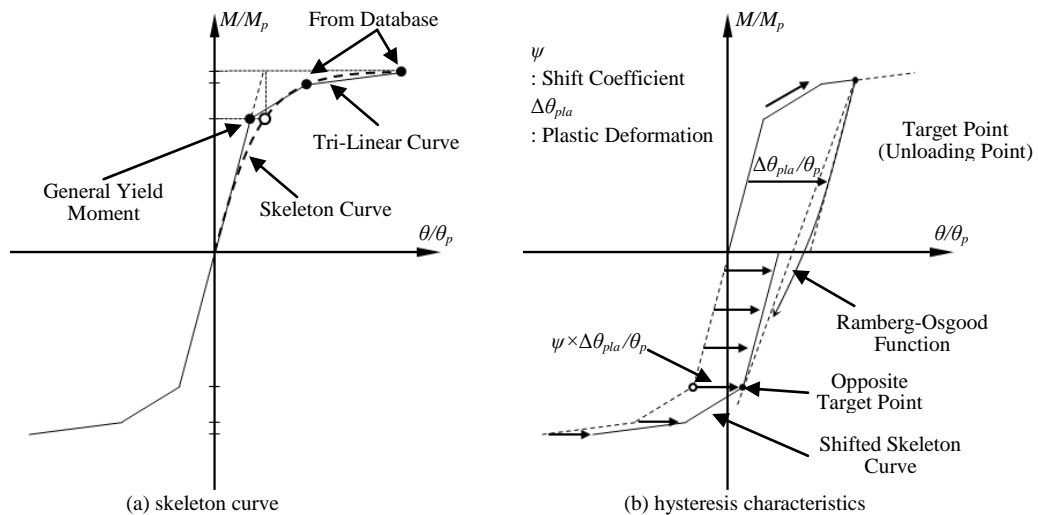


**Figure 5.1.** Skeleton curve and hysteresis rule of the Skeleton Shift Model

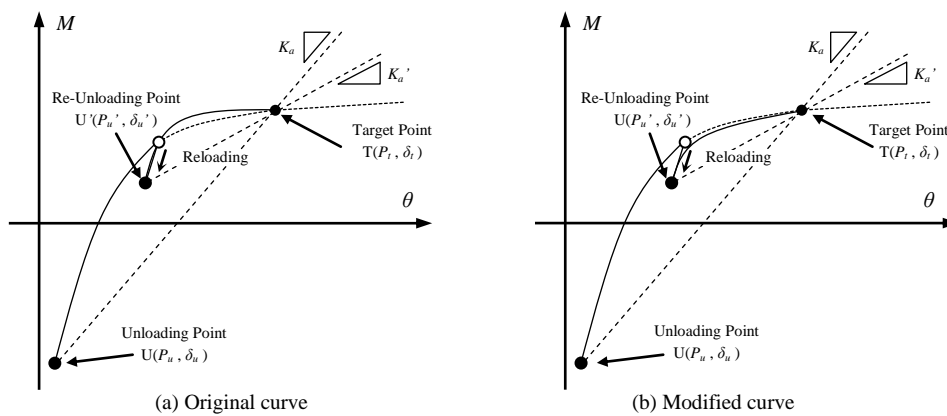


**Figure 5.2.** Hysteresis curve during unloading process

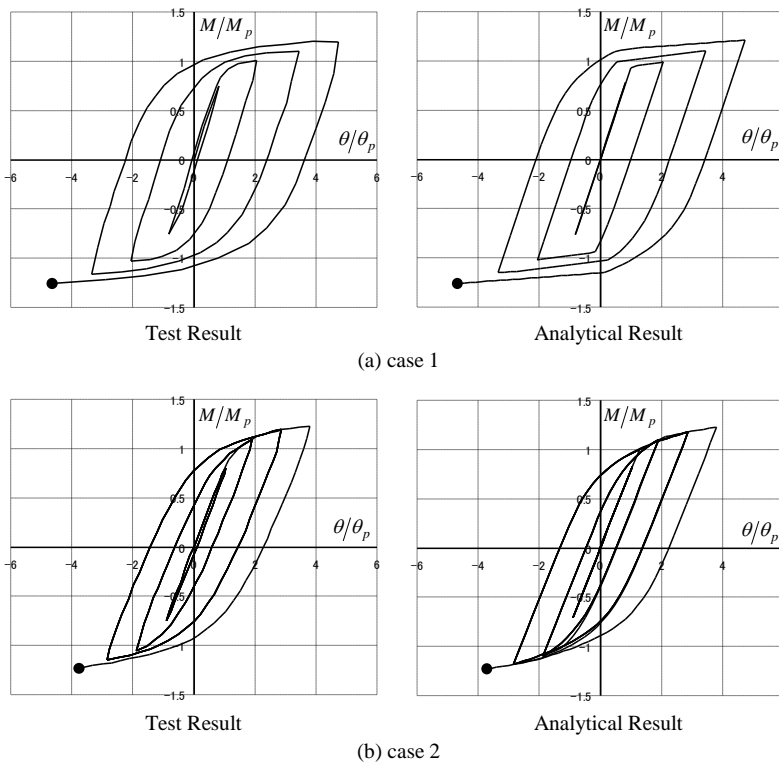


**Figure 5.3.** Comparison of test and analysis in hysteresis loop

## 6. CONSLUSION

In this paper, the cumulative damage index, which predicts the ductility at the maximum strength of the steel beam subjected to cyclic loadings, was formulated by the references in the database of a large number of past references. This index has good agreements with the test results in the database. And also, this paper proposed the analytical method, the restoring force and hysteresis model of steel beams subjected to cyclic loadings. To compare the analytical simulation with the test results of the database, the proposed methods and model can simulate effectively the ultimate states of steel beams.

## REFERENCES

- Meng L. Ohi, K., and Takanashi, K. (1992). A simplified model of steel structural members with strength deterioration used for earthquake response analysis. *Journal of structural and construction engineering*. **No437:**, 115-124
- Ramberg, W. and Osgood, W. R. (1943). Description of stress-strain curves by three parameters. *National Advisory Committee on Aeronautics*. **Technical Note 902:**.